Temporal and geographical variation in body condition of common minke whales (*Balaenoptera acutorostrata acutorostrata*) in the Northeast Atlantic

H. K. Solvang (corresponding author)
Institute of Marine Research, PO Box 1870 Nordnes, N-5817 Bergen, Norway
e-mail: hiroko.solvang@imr.no

H. Yanagihara
Department of Mathematics, Graduate School of Science, Hiroshima University, Higashi-Hiroshima 739-8526, Japan

N. Øien
Institute of Marine Research, PO Box 1870 Nordnes, N-5817 Bergen, Norway

T. Haug
Institute of Marine Research, PO Box 6404, N-9294 Tromsø, Norway

Abstract: The common minke whale (*Balaenoptera acutorostrata acutorostrata*) is a boreo-arctic species, and the summer period is generally characterized by intensive feeding and consequently seasonal fattening at high latitudes. The fat deposited is stored as energy reserves for overwintering at lower latitudes where feeding is greatly reduced. It is therefore expected that their body condition on the summer grounds will reflect food availability during their most intensive feeding period and thus indicate how well the high latitude ecosystems can support the populations. During the commercial catch operations on feeding grounds in Norwegian waters, body condition data (blubber thickness and girth) have been collected from 10,556 common minke whales caught from 1993 to 2013. To investigate associations between condition and time/area, we applied the following three models: 1. Multiple regression models with covariates; sex, year, latitude and longitude to find significant coefficients of the covariate; 2. Random effect models involving the random effects of variations by year or area and with sex as a fixed variable; 3. Varying coefficients models (VCMs) which were applied to investigate variation with year/area and to interpret covariate effects by visualizations. The significance of the estimated coefficients can be assessed by statistical tests. In conclusion, the total trend over the two decades of data available suggests a decrease in minke whale condition. However, this trend was most pronounced during the high summer season when we considered the seasonal effect over the annual sampling periods from April to September.

Keywords: Northeast Atlantic · minke whales · body condition · varying coefficients modelling · temporal variation · geographical variation

Introduction

Current knowledge of the distribution of common minke whales (*Balaenoptera acutorostrata acutorostrata*) in the North Atlantic is based upon records of catches, sightings, and strandings. It is suggested that the species inhabit temperate and tropical waters during winter, and recordings have been made as far south as c. 16°N on the western side (Mitchell 1991), c. 14°N on the eastern side (Van Waerebeek 1999) and 10°40'N in the offshore northeast Atlantic (Folkow and& Blix 1991). Births and mating takes place during winter (Jonsgård 1951), whereas a general feeding migration to higher latitudes occurs in spring and early summer, after which the animals return to lower latitudes in the autumn (Jonsgård 1966). The feeding grounds range from the Canadian East Coast to the Novaya Zemlya region of the Russian western Arctic during summer (*e.g.* Stewart and Leatherwood 1985). During this time of the year they seem to be mainly limited to continental shelf areas although they are also found in offshore deep-water areas, and their distribution is more or less continuous from the eastern and central parts of the North Atlantic to West Greenland (Horwood 1990; Donovan 1991). The migration into Norwegian waters starts in early spring and there are probably at least two paths followed (Haug et al. 2011): One from southwest through the Norwegian Sea and one along the Norwegian coast. There is apparently a migration route along the coast of northern Norway into the Barents Sea in early summer, and then later in the summer a return is made westwards and ending up at Spitsbergen. In September-October a southward migration has been observed.

As most mysticetes the common minke whale is a boreo-arctic species (Jonsgård 1966), and the summer period is generally characterized by intensive feeding and consequently seasonal fattening, while feeding in the rest of the year is generally considered to be greatly reduced (Lockyer 1981; Næss et al. 1998). The fat deposited is stored as energy reserves for overwintering at lower latitudes where reproduction takes place. In the North Atlantic, also fin whales (*Balaenoptera physalus*) and sei whales (*Balaenoptera borealis*) have been demonstrated to exhibit seasonal variation in body condition and relative amounts of body fat (Lockyer et al. 1985; Lockyer 1986; Lockyer and Waters 1986; Vikingsson 1990; 1995).

Common minke whales have a flexible foraging behaviour and are normally able to switch among species without compromising the body condition. As a result their diet varies much in time (year and season) and space due to spatio-temporal variation in prey availability (Haug et al. 2002; Windsland et al. 2007). The whales exploit a variety of species and sizes of fish and crustaceans, however they appear to selectively forage on capelin, herring and occasionally krill (Lindstrøm and Haug 2001). Nevertheless, relationships have been observed between minke whale body condition and ecological changes in their feeding areas. In the Barents Sea, Haug et al. (2002) observed that common minke whales were in poor condition in years with low habitat quality, primarily caused by insufficient availability of herring (*Clupea harengus*) and capelin (*Mallotus villosus*). Antarctic minke whales *Balaenoptera bonarensis* have exhibited a prevailing decrease in body condition over nearly two decades (Konishi et al. 2008), presumably due to a combination of reduced krill availability and/or increased abundance of krill feeders other than minke whales in the area (see Mori and Butterworth 2006).

Cod (*Gadus morhua),* harp seals (*Pagophilus groenlandicus*) and common minke whales are the main top predators in the Barents Sea (Bogstad et al. 2015). As for the minke whales, also harp seal body condition is characterized with seasonal fattening during an intensive feeding period during summer and autumn (Nilssen et al. 1997). There is also good evidence to suggest that, in addition to this seasonal variation, there is interannual variation in the body condition of harp seals resulting from changes in prey abundance (Timoshenko 1995; Chabot et al. 1996; Nilssen et al. 1997; 2001; Øigård et al. 2013). The Barents Sea ecosystem has undergone substantial ecological fluctuations over past 3-4 decades, and Øigård et al. (2013) have shown that harp seal body condition, estimated from samples taken during spring in 1992-2011, exhibited a slow increase from 1992 to 2001, where after a significant decrease to a minimum in 2011 has occurred. The main question addressed in this paper is whether also common minke whales exhibit interannual, and potentially also geographical variation, in body condition in response to temporal and regional variations in the Barents Sea and other Northeast Atlantic ecosystems in which they feed and are harvested.

Sampling during scientific whaling operations under special permit in 1993-1994 (see Haug et al. 1996) and commercial whaling operations in 1993-2013 have provided a time series of minke whale body condition data which may serve as a tool to address these questions. The data collected include year, month (May to September), day, latitude / longitude, sex, girth and three blubber thickness measurements. We use the blubber thickness measured at three specific sites and the girth as describing the body condition. To investigate association between these data and time/area, we applied the following three models: 1. Multiple regression models with covariates; sex, year, latitude and longitude to find significant coefficients of the covariate; 2. Random effect model involving the random effects of variations by year or area and with sex as a fixed variable; 3. Varying coefficients models (VCMs) were applied to investigate variation with year/area and to interpret covariate effects by visualizations. The VCM is represented by combinations of polynomial expressions for year and area, which represent the variation of them. The VCMs include terms to predict more complicated variations between year and areas. Originally, West et al. (1985) and Hastie and Tibshirani (1993) proposed to formulate VCMs according to time as a regression analysis applied to longitudinal data. The VCMs can be used for visualizations or interpretations of the effects of fluctuating covariates. In this study, we propose a statistical testing method to assess whether estimated VCMs are significant.

Material and methods

Field work

Over the period 1993-2013, body condition data were obtained from a total of 10 556 common minke whales taken in Norwegian scientific and commercial whaling operations in the Northeast Atlantic (Fig. 1) during the months April to September (Table 1).

Immediately after death, the whales were taken onboard and hauled across the fore-deck of the boat. Total body length was measured in a straight line from the tip of the upper jaw to the apex of the tail fluke notch; girth was measured right behind the flipper; and blubber thickness was measured at three sites (Fig. 2): Dorsally behind the blowhole (BT1) and behind the dorsal fin (BT2), and laterally just above the centre of the flipper (BT3). Blubber measurements were made perpendicular from the skin surface to the muscle–connective tissue interface. Length and girth measurements were made to the nearest centimeter, while blubber measurements were to the nearest millimeter. The above morphometric measurements are identical to those referred to as G1 (girth) and D8/D11/L5 (blubber) in the comprehensive work by Næss et al. (1998). For all whales, the year, month, day, latitude and longitude were recorded. Total number of individuals was 10,556. After removing missing data, final numbers of individuals that were included in the analyses were 10,207 for BT1, 10,203 for BT2, 10,199 for BT3 and 10,303 for the girth.

Data preprocessing

We corrected the effect of body length on the girth measurements as described by Haug et al. (2002), i.e., as an index based on residuals from the girth – body length regression:

Girth index = girth value – (intercept + coefficient × body length)

The intercept of the regression model was 15.4 and the estimated coefficient for the length was 0.46 as a girth index. The p-values for these estimations were < 5.0e-16 and Cohen's effect size (Cohen 1988) was 1.29, indicating an effect of body length on girth. Blubber thickness measurements were tested for possible effects of body length as well, and the estimated regression coefficients for BT1, BT2 and BT3 were quite small, 0.04, 0.18 and 0.03, respectively. Very small p-values (around 2.0e-16) for these estimations were obtained, probably caused by large sample sizes. Cohen's effect sizes indicated 0.18, 0.38 and 0.13, respectively. Therefore, we decided not to correct for effect of body length in the analysis of blubber thickness.

Statistical analyses

We applied three regression models to the body condition data with relevant covariates:

1. Ordinary linear regression model

To investigate linear associations, we applied an ordinary multiple regression model (OLM) to the data (total N):

$$y_i = \alpha + \mathbf{X}_i\boldsymbol{\beta} + \varepsilon_i^{\mathrm{OL}} \text{ for } i = 1, \cdots, N,$$

where y_i, α, $\mathbf{X}_i$, $\boldsymbol{\beta}$ and $\varepsilon_i^{\mathrm{OL}}$ indicate variables for body condition, intercept, covariates, coefficients and prediction error with mean zero and unknown variance σ_{OL}^2, respectively. The computational program used applied the lm function in the R package;

2. Random effect model for year and location

To consider possible temporal or geographical effects, we applied a random effect model (REM) for year and location to body condition:

$$y_i = \alpha + \mathbf{X}_i\boldsymbol{\beta} + \mathbf{V}_i\mathbf{b}_i + \varepsilon_i^{\mathrm{RE}} \text{ for } i = 1, \cdots, N,$$

where $\boldsymbol{\beta}$ is the fixed effect shown in the ordinary linear model, $\mathbf{V}_i$ corresponds to variables with random effect and $\mathbf{b}_i$ follows a normal distribution with zero mean and unknown variance-covariance matrix Σ , and $\varepsilon_i^{\mathrm{RE}}$ indicate the prediction error with zero mean and another unknown variance σ_{RE}^2 . The computational program used applied the lmer function in the R package 'lme4'. The random effects cannot be directly assessed by the estimates of REM. For this reason, the conditional means of the model were considered. These values were calculated by the *ranef* function in R.

3. Varying coefficients model (VCM)

The VCM in this study is represented by combinations of polynomial expressions for year and area, which describe their variation:

$$y_i = \alpha + \mu_p(t_i) + \gamma_q(\mathrm{v}_i, u_i) + \mathbf{X}_i\boldsymbol{\beta} + \varepsilon_i^{\mathrm{VC}} \text{ for } i = 1, \cdots, N ,$$

where α is an intercept of this model, $\mu_p(t_i)$ and $\gamma_q(v_i, u_i)$ correspond to varying coefficients related to functions for year and area (longitude v_i latitude u_i), and $\varepsilon_i^{\mathrm{VC}}$ indicates prediction error with zero mean and unknown variance σ_{VC}^2 . In general, any non-parametric function is available for varying coefficients (VC) to obtain smoothing curves for random fluctuations. Here, we describe p- and q-dimensional multiple polynomials for these terms as:

$$\mu_p(t_i) = \mu_1 t_i^1 + \mu_2 t_i^2 + \cdots + \mu_p t_i^p$$

$$\gamma_q(v_i, u_i) = \gamma_{1,1} v_i + \gamma_{1,2} u_i + \cdots + \gamma_{q,1} v_i^q + \gamma_{q,2} v_i^{q-1} u_i + \cdots + \gamma_{q,q} v_i u_i^{q-1} + \gamma_{q,q+1} u_i^q$$

where μ_* indicates the coefficient for year t_i and $\gamma_q(v(t_i), u(t_i))$ is represented by q-dimensional polynomial for longitude $v(t_i)$ and latitude $u(t_i)$ at the year t_i . Using estimated coefficients, we can describe VC curves for $\mu_p(t_i)$ and $\gamma_q(v_i, u_i)$ to observe possible fluctuations in body condition. Furthermore, we propose a statistical test to assess whether variations in year and area to body condition are significant. The theoretical details are shown in the Appendix. The computational program applied is simply the lm function in the R package.

As a model similar to VCM, a generalized additive model (GAM) has also been proposed for cases like this (Hastie and Tibshirani 1990). The model includes non-linear smoothing terms that correspond to μ_p or γ_q in VCM. For the parameter estimation for GAM, a numerical optimization should be performed. This is time consuming, depending on the number of parameters involved. Unlike this, VCM is used by just least squares method to estimate all parameters and computation is faster even if the numbers of parameters increase.

The above models were considered for all possible combinations of relevant covariates. To select the best fit for various model candidates, we used a Bayesian information criterion (BIC) defined by

$$\text{BIC} = -2 \times \text{log-likelihood} + \#\ \text{model parameters} \times \log(N)\,.$$

By minimizing BIC, model parameters $\left(\hat{\boldsymbol{\beta}}, \hat{\sigma}^2_{\text{OL}}\right)$ for OLM, $\left(\hat{\boldsymbol{\beta}}, \hat{\mathbf{b}}, \hat{\Sigma}, \hat{\sigma}^2_{\text{RE}}\right)$ for REM and $\left(\hat{\mu}_1, \cdots, \hat{\mu}_p, \hat{\gamma}_{1,1}, \cdots, \hat{\gamma}_{q,q+1}, \hat{\boldsymbol{\beta}}, \hat{\sigma}^2_{\text{VC}}\right)$ for VCM were obtained. The coefficients of OLM and VCM were assessed by t-tests where the p-values turned out to be small due to large sample size. Therefore, we also calculated Cohen's effect size which was around 0.02, 0.15 and 0.35, thus indicating small, medium and large effects from the estimated covariates to the null model.

Results

General temporal patterns of the data

The general patterns of the body condition data, pooled by catch season, with confidence intervals for each year are shown in (Fig.3). The means for the four measurements over all data are: BT1=38.5 cm (standard deviation (SD)= 10.3), BT2=132.4 (SD=32.9) , BT3= 34.9 (SD=9.1) and Girth=357.7 (SD=50.65). BT1 and BT3 showed a negative tendency during the period of observations, while BT2 and Girth showed more random fluctuation with year.

Regression analyses

Applying OLM, REM and VCM, we have summarized the calculated log-likelihood, and BIC for the different covariate combinations in Table 2. The model selected by minimum BIC is marked by *. Estimated coefficients of OLM, variances of REM and test statistics for VCM are summarized in Table 3. The analysis by OLM indicated that both covariates year and area associated significantly with BT1 and BT3, while only the covariate area associated significantly with BT2 and Girth (all p-values > 6.8e-04 for estimated coefficients and effect size for those models was in the range 0.04 – 0.11). In the case of REM, the model with random effect of year and area was selected as the best model for all data. Estimated variances for years were larger than for areas for BT1 and BT3. BIC values for the best REMs were larger than those for the best OLMs, except for BT2. VCM with p=2 and q=3 for BT1 was selected as the best model for BT1, VCM with p=2 and q=2 was best for BT2 and Girth, and VCM with p=3 and q=2 was best for BT3. All proposed statistical tests for the estimated VCs indicated significance for both year and area, and the effect sizes for the best VCMs were in the range of 0.05 – 0.13.

Seasonal effect

Based on Næss et al. (1998) we assumed that body condition data involve seasonal variations, and considered three season categories where I combined April and May, II combined June and July, and III combined August and September (Fig. 4). The fluctuations for BT2 and Girth exhibited similar trends in season II. BT1 and BT3 indicated clear negative trends with year in season II, while for seasons I and III the trends were much more vague.

To confirm whether seasonal effect should be included in the model, we consider adding dummy variables where

$d1 = 1$ for season I

$d2 = 1$ for season III

intercept for season II

as seasonal effect into the best models for OLM, REM and VCM. The formula, e.g., in the case of OLM, is represented by $y_i = \alpha + \mathbf{X}_i\boldsymbol{\beta} + d1 + d2 + \varepsilon_i^{\mathrm{OL}}$. We added the likelihood and BIC for this model on the row named 'Best model + d1 + d2' in Table 2. And we observed that seasonal effect contributed to better predictions except in one case, OLM of BT1.

For BT1 and BT3, where clear trends were indicated in season II, we applied three regression models and the results are summarized in Table 4. Estimated coefficients for covariates, variances for random effect and test statistics for VCM are shown in Table 5. The minimum BIC model for OLM included covariates for year and area that were all significant. Estimated variance for random effect of year was larger than those variances of area. The best fitted model among the three models used was VCM for both year and area. The statistical test established significant VCs for year and area, and the effect sizes of the best VCM for BT1 and BT3 were 0.12 and 0.10, respectively.

The conditional mean values are shown in Fig. 5. The plots for random effects of year genearlly followed the changes of mean levels for the original data set as shown in Fig. 3. The plots for random effects of latitude and longitude are illustrated on the x-axis.

Estimated VC curves are illustrated in Fig. 6. The curves for year (with confidence intervals) exhibited negative trends. The contour plots of VC are shown for longitudes (x-axis) and latitudes (y-axis). The change in color from yellow to red correspond to a change from poor to good body condition, and the data indicate a gradient with better body condition in the northeast tnhan forther to the west and south.

Discussion

This study indicates that the blubber thickness in common minke whales captured in Norwegian waters, varied over the years. A time series of consistent blubber measurements, sampled during commercial whaling in the period 1993-2013, showed a significant negative trend over the entire period with particular low values in 2011-2013. The trend was clearer in midsummer (June-July) than in autumn (August-September) and spring (April-May).

The body condition data analyzed were recorded at four different sites on the whale body (Fig. 2), but the trend showing more or less continuous decrease with time was not equally evident in all four. While the decrease was clear in two of the blubber thickness measurements (BT1, taken dorsally behind the blow hole, and BT3, taken laterally just above the centre of the flipper), neither the girth nor the blubber thickness measurement made behind the dorsal fin (BT2) did show equally conclusive patterns. In fact, both these measurements exhibited more stable trends, however with short periods of drops in level (1994 for the girth, 2003-2005 for both). It should be noted that in the area behind the dorsal fin, where BT2 was measured, the local variation in blubber thickness is quite large between the actual spot and close neighboring areas on the whale body. Therefore, it is more difficult to obtain consistent measurements between individuals at this spot as compared with BT1 and BT3 where the blubber thickness is the same over larger areas of the whale body. Also, girth was measured as half of the circumference and then this measurement was doubled. As a result, BT2 and girth potentially included more measurement errors, and became more variable and unreliable than BT1 and BT3.

From the estimated random effect by area (latitude) shown in Fig.5, there were some apparent common features. At latitudes around 60° and 70° - 75° N, the random effect was positive. These locations were the North Sea and Finnmark-Svalbard, respectively, both known as important feeding grounds for common minke whales (Haug et al. 2002; Windsland et al. 2007). Also, a positive random effect around 65° N could be related to feeding on herring in the Norwegian Sea (Windsland et al. 2007). On the other hand, a negative random effect around 68° N could be related to an area near Lofoten where lean individuals first arrived early in the season to start feeding (see Haug et al. 2011). Furthermore, we saw a positive random effect around -10° E (longitude) which was located in the herring areas of the Norwegian Sea.

Haug et al. (2002) and Windsland et al. (2007) observed that common minke whales had a flexible foraging behaviour and were normally able to switch among species without compromising the body condition. As a result their diets varied much in time (year and season) and space due to spatio-temporal variation in prey availability (see also Bogstad et al. 2015). The whales exploited a variety of species and sizes of fish and crustaceans, but they appeared to selectively forage on capelin, herring and occasionally krill (Lindstrøm and Haug 2001). In extreme events, such as in the Barents Sea in 1995-1996, when the abundances of capelin and herring were low simultaneously, the common minke whales had to switch to krill and gadoid fish and as a result their body condition declined (Haug et al. 2002). Changes in body fattening, which could be related to food availability, have been observed also for fin whales in Icelandic waters between 1977 and 1982 (Lockyer 1986) and for Antarctic minke whales between 1990 and 1995 (Ichii et al. 1998). Konishi et al. (2008) observed that blubber thickness, girth and fat weight had been decreasing significantly in Antarctic minke whales over the entire period from 1987 to 2005, presumably due to a combination of reduced krill availability and/or increased abundance of krill feeders other than minke whales in the area (Mori and Butterworth 2006).

The ecosystems sustaining common minke whales with food have undergone changes over the past two decades. This is also true for key prey species for common minke whales, including for example krill. The production and standing stocks of zooplankton is difficult to monitor, and there are probably spatial shifts and geographical variation that are difficult to trace, but may be important when considering the importance of this prey group for top predators (Bogstad et al. 2015). In the Barents Sea, krill abundance estimated during autumn (October-December) is at present at, or slightly above, the long-term mean (McBride et al. 2014), and krill abundance estimates from the annual joint Norwegian Russian ecosystem surveys (Prokhorova 2013) also indicate that krill abundance in the last decade has been above average in the area. In the Norwegian Sea there have been a change in distribution and reduction in biomass of krill (and other macrozooplankton species) over the last 10-15 years, and Nøttestad et al. (2015) observed that minke whales are now significantly associated with herring, but not correlated with krill in the area.

Capelin is a very important forage fish species for top predators (including common minke whales) in the Barents Sea, despite major fluctuation in stock size. The biomass has historically been estimated to exceed seven million tonnes, however, on three occasions during the last 2 decades (1993-1997 and 2003-2007), the stock dwindled and reached a level two orders of magnitude lower (Bogstad et al. 2015). In cold years the capelin stock is normally distributed to the north of the polar front during autumn, and in periods it has extended to the ice edge. In current warm years, capelin have been observed both south and north of the shelf edge, i.e. north of the Svalbard and Franz Josef Land archipelagos at 81˚N (Ingvaldsen and Gjøsæter, 2013). The general retraction of the ice edge northwards during the last decades may have opened up new areas both for primary and secondary producers, and there are indications from the joint Norwegian Russian ecosystem surveys that macrozooplankton is now more abundant in the marginal northern areas than centrally in the Barents Sea (Michalsen et al. 2013). There is a negative relationship between the amount of capelin and macrozooplankton such as krill, explained as a direct effect of variable grazing pressure from capelin (Dalpadado and Skjoldal 1996). The lack of zooplankton in central areas may, therefore, be caused by grazing by the large capelin stock. Common minke whales may benefit from the increased plankton stocks in the north, and observations from the ecosystem surveys suggest that they probably have moved northwards and taken advantage of these resources in several years already (Skern-Mauritzen et al. 2011).

The southern Barents Sea serve as the main nursery area for immature herring of the Norwegian spring spawning stock (Dragesund et al. 1997). Good recruitment to this stock gives strong cohorts and large abundance of immature (0-3 years old) herring in the area. Upon attainment of maturation, however, the herring migrate westwards out of the Barents Sea and into the Norwegian Sea where they join the adult stock. Recruitment failure with subsequent weak cohorts or low larval survival will, therefore, reduce the abundance of young herring in the southern Barents Sea. Considerable variation in herring recruitment have been observed during the two most recent decades, and particularly strong cohorts gave subsequent good abundance on the nursery areas in 1992-1994, 1999-2001 and 2003-2006 (Bogstad et al. 2015). The absence of strong year classes (and subsequent good availability of juveniles in the southern Barents Sea) after 2006 have also resulted in a substantial decrease in the adult herring stock in the Norwegian Sea after 2009 (Nøttestad et al. 2015).

Evidently, there has not been a situation with simultaneous low abundance of both herring and capelin in the Barents Sea after the event that caused declined common minke whale body condition in 1995-1996 (see Haug et al. 2002). Also there are no clear signals of zooplankton declines in this area in recent years, while the opposite seems to be the case in the Norwegian Sea where also the herring stock has dwindled. Traditionally, however, the Norwegian Sea has primarily been an important migration corridor for minke whales heading towards feeding grounds further to the east and north, and to a lesser extent vital as a feeding ground for the species which has been observed in lower numbers in the area in the most recent decade (Nøttestad and Olsen 2004; Nøttestad et al. 2015). Nevertheless, there are signals in the current study (Figs 5 and 6) indicating feeding, presumably on herring, in the Norwegian Sea and the possibility cannot be excluded that reduced habitat quality in the Norwegian Sea may have contributed to the observed decline in common minke whale condition. A tremendous increase in mackerel has occurred in the Norwegian Sea during the past decade, but although we know that the species is taken by common minke whales in the North Sea (Windsland et al. 2007) there is no evidence that mackerel is important whale food further to the north (Bogstad et al. 2015; Nøttestad et al. 2015).

The Barents Sea cod stock is currently at record high level, and the distribution of the stock has expanded north and northeastwards during the last decade (Bogstad et al. 2015). The distributions of cod, particularly medium and large individuals, and minke whales overlap to various degree during the year. The most intensive spatial overlap between the two predators occurs during summer and autumn in the central and northern parts of the Barents Sea, i.e., the main area for the Norwegian common minke whale hunt and therefore also the sampling for this study. Given our dietary knowledge of these predators they may well compete for krill as well as capelin in these periods (Haug et al. 2002; Johannesen et al. 2013). A recent study focussed on the intra- and interspecific competition among top-predators (cod, common minke whale and sea birds), and concluded that common minke whales and cod competed for food and that their diets depended on the abundance of herring and capelin, respectively (Durant et al. 2014). Apparently, it may look as if the common minke whale is paying a price for having a big cod stock by declining body condition over the past two decades. Similar observations have been made in Barents Sea harp seals where there is a negative trend in body condition in the most recent decade (Øigård et al. 2013). In their review of the battle for food among common minke whales, harp seals and cod in the Barents Sea, Bogstad et al. (2015) suggested that the decreased body condition in the two mammal stocks might be an indication that they had simply been outperformed by the record high cod stock.

When common minke whales arrive on their northern feeding grounds in spring they are extremely lean, but during their stay they gain considerable fat reserves which they deposit in the blubber layer, particularly during late summer and autumn (July-September, Næss et al. 1998). This reflects the dynamics of lipid transfer in the Arctic marine ecosystems, where the energy produced during the algal bloom is transferred up through the food chain during summer and autumn to top predators, such as whales (Falk-Petersen et al. 1990; 2009). Feeding is the reason why common minke whales migrate northwards every spring, attracted by the good availability of particularly high energetic food in the northern areas. Their preference for krill in the diet, particularly early in the season when these crustaceans are much more lipid-rich than any of the preferred fish prey species (see

Grahl-Nielsen et al. 2011), seems very logical. However, a gradual shift in species composition towards more Atlantic dominated zooplankton species which has been observed in the northern areas during the past decade (Dalpadado et al. 2012) implies that high energy dense arctic ice-associated prey is being replaced by Atlantic species which are less energy dense (Wassmann et al. 2006; Falk-Petersen et al. 2007). The outcome of this change is difficult to predict but, in general, if this leads to less energy-rich food available in the customary feeding areas of the common minke whales, their ability to build up energy deposits during the feeding season may be compromised and affect their ability to undertake long migrations to breeding areas and to suckle their young.

Appendix

We show theoretical details of statistical procedures of a varying coefficient model when a varying coefficient $\beta(z)$ is expressed as $\beta(z) = \boldsymbol{x}(z)'\boldsymbol{\theta}$ (see e.g., Satoh and Yanagihara 2010), where $\boldsymbol{x}(z)$ is a s-dimensional vector of basis functions for a varying coefficient, $z = (z_1, ..., z_p)'$ is a p-dimensional vector of covariates for a varying coefficient, and $\boldsymbol{\theta}$ is a s-dimensional vector of unknown parameters. If we consider a time-varying coefficient model, then $p = 1$ and $z_1 = time$ (or $year$), and if we consider a space-varying coefficient model, then $p = 2$ and $(z_1, z_2)' = (longitude, latitude)'$, and if we consider a time-space-varying coefficient model, then $p = 3$ and $(z_1, z_2, z_3)' = (year, longitude, latitude)'$. If we express a trend of varying coefficient by a cubic polynomial, then $s = 4$ and $\boldsymbol{x}(z) = (1, z, z^2, z^3)'$. Statistical procedures written here are derived by modifying those in Tonda and Satoh (2013). Suppose that the estimator of $\beta(z)$ denote $\hat{\beta}(z) = \boldsymbol{x}(z)'\hat{\boldsymbol{\theta}}$, and the variance of $\hat{\beta}(z)$ denote $\lambda(z)^2$. We define

$$T(z) = \frac{\{\hat{\beta}(z) - \beta(z)\}}{\lambda(z)}.$$

Let $z_i = (z_{i1}, ..., z_{ip})'$ be z of an ith individual ($i = 1, ..., N$), where N is the sample size, and $\mathcal{A}$ be a region of z satisfying $z_1, ..., z_n \in \mathcal{A}$. A simple example of $\mathcal{A}$ can be defined as $\mathcal{A} = J_1 \times \cdots \times J_p$, where

$$J_c = \left\{ x \in \mathbb{R} \,\middle|\, z_{c,1} = \min_{i=1,..,n} z_{ic} \le x \le \max_{i=1,..,n} z_{ic} = z_{c,2} \right\}, \ (c = 1, ..., p),$$

and the notation "$\times$" denotes a direct product of a set. Then, we evaluate $1-\alpha$ confidence interval of $\beta(z)$. In order to evaluate it, we have to calculate τ_α such that $\Pr(T \le \tau_\alpha) = 1-\alpha$, where

$$T = \sup_{z \in \mathcal{A}} |T(z)|.$$

Let $\boldsymbol{a}_1, ..., \boldsymbol{a}_K$ be p-dimensional vectors included in $\mathcal{A}$. As for an example of $\boldsymbol{a}_1, ..., \boldsymbol{a}_K$ when $p = 2$, e.g., $\boldsymbol{a}_k = (a_{k1}, a_{k2})'$ ($k = (q-1)m + r;\ 1 \le q \le m,\ 1 \le r \le m$), where m is some integer, and

$$a_{k1} = z_{1,1} + \frac{(q-1)(z_{1,2}-z_{1,1})}{m}, \quad a_{k2} = z_{2,1} + \frac{(r-1)(z_{2,2}-z_{2,1})}{m}.$$

For K large enough, T can be approximated by

$$T \approx T_{\max} = \max_{k=1,\dots,K} \left|T(\boldsymbol{a}_k)\right| = \max\left\{\left|T_1\right|,\dots,\left|T_K\right|\right\},$$

where $T_k = T(\boldsymbol{a}_k)$. Hence, we have

$$\Pr(T \le \tau_\alpha) \approx \Pr(|T_1| \le \tau_\alpha, \dots, |T_K| \le \tau_\alpha),$$

On the other hand, it is known that

$$(T_1,\dots,T_K)' \xrightarrow{d} N_K(\boldsymbol{0}_K, \boldsymbol{R}) \ as\ n \to \infty,$$

where $\boldsymbol{0}_K$ is a K-dimensional vector of zeros, and $\boldsymbol{R}$ is a $K \times K$ matrix defined by

$$\boldsymbol{R} = \boldsymbol{DC\Omega C'D},\ \boldsymbol{C} = \left(\boldsymbol{x}(\boldsymbol{a}_1),\dots,\boldsymbol{x}(\boldsymbol{a}_K)\right)',\ \boldsymbol{D} = \mathrm{diag}\left(\lambda(\boldsymbol{a}_1),\dots,\lambda(\boldsymbol{a}_K)\right)^{-1},$$

and $\boldsymbol{\Omega}$ is the covariance matrix of $\hat{\boldsymbol{\theta}}$. This implies that the threshold τ_α can be obtained by multivariate normal distribution. Practical procedures for the test is that: 1) the differentiated coefficients, the estimated covariance matrix and $\mathrm{H}_0 : \beta(\boldsymbol{z}) = 0$ are set on $T(\boldsymbol{z})$, i.e., $T_h(\boldsymbol{z}) = \hat{\beta}(\boldsymbol{z}) / \lambda(\boldsymbol{z})$, 2) calculate the threshold τ_α by the multiple integral of multivariate normal distribution (qmvnorm function in R package *mvtnorm*) using the covariance matrix, and 3) Compare τ_α and $T_{h,\max} = \max\{T_h(\boldsymbol{a}_1),\dots,T_h(\boldsymbol{a}_K)\}$. If $T_{h,\max} > \tau_\alpha$, H_0 should be rejected.

References

Bogstad B, Gjøsæter H, Haug T, Lindstrøm U (2015) A review of the battle for food in the Barents Sea: Cod vs marine mammals. Front Ecol Evol 3:29. doi: 10.3389/fevo.2015.00029

Chabot D, Stenson GB, Cadigan NG (1996) Short- and long-term fluctuations in the size and condition of harp seal (*Phoca groenlandica*) in the Northwest Atlantic. NAFO Sci Coun Studies 26:15-32

Dalpadado P, Ingvaldsen RB, Stige LC, Bogstad B, Knutsen T, Ottersen G, Ellertsen B (2012) Climate effects on the Barents Sea ecosystem dynamics. ICES J Mar Sci 69: 1303-1316. Doi: 10.1093/icesjms/fss0

Dalpadado P, Skjoldal HR (1996) Abundance, maturity and growth of the krill species *Thysanoessa inermis* and *T. longicaudata* in the Barents Sea. Mar Ecol Prog Ser 144: 175-183

Donovan GP (1991) Distribution of sightings of minke whales in the North Atlantic. Appendix 5. Rep Int Whal Commn 41: 150-151

Dragesund O, Johannessen A, Ulltang Ø (1997) Variation in migration and abundance of Norwegian spring spawning herring (*Clupea harengus* L.). Sarsia 82: 97-106

Durant J, Skern-Mauritzen M, Krasnov YV, Nikolaeva NG, Lindstrøm U, Dolgov AV (2014) Temporal Dynamics of Top Predators Interactions in the Barents Sea. Plos One 9:11. doi:10.1371/journal.pone.0110933

Falk-Petersen S, Haug T, Hop H, Nilssen KT, Wold A (2009) Transfer of lipids from plankton to blubber of harp and hooded seals off East Greenland. Deep-Sea Res II 56: 2080-2086

Falk-Petersen S, Hopkins CCE, Sargent JR (1990) Trophic relationships in the pelagic, Arctic food web. In: Barnes M, Gibson RN (eds) Trophic relationship in the marine environment. University Press, Aberdeen, pp 315-333

Falk-Petersen S, Timofeev S, Pavlov V, Sargent JR (2007) Climate variability and the effect on arctic food chains. In: Ørbæk JB, Kallenborn R, Tombre I, Hegseth E, Falk-Petersen S, Hoel AH (eds). Arctic-alpine ecosystems and people in a changing environment. Springer, Berlin, Heidelberg, New York, pp 147-161

Folkow LP, Blix AS (1991) Norwegian whale sighting and acoustic surveys in the Atlantic Ocean during the winter of 1989/90. Rep Int Whal Commn 41:31-538

Grahl-Nielsen O, Haug T, Lindstrøm U, Nilssen KT (2011) Fatty acids in harp seal blubber do not necessarily reflect their diet. Mar Ecol Prog Ser 426: 263-276

Hastie T, Tibshirani R (1990) Generalized Additive Models. Monographs on Statistics and Applied Probability 43. Chapman & Hall/CRC.

Hastie T, Tibshirani R (1993) Varying-coefficient models. J Roy Stat Soc, Ser B 55: 757-796

Haug T, Bjørge A, Øien N, Ziryanov SV (2011) 7. Marine mammals. In: Jakobsen T, Ozhigin VK (eds). The Barents Sea; Ecosystem, resources, management; Half a century of Russian-Norwegian cooperation. Tapir Academic Press, pp 395-430

Haug T, Lindstrøm U, Nilssen KT (2002) Variations in minke whale (*Balaenoptera acutorostrata*) diet and body condition in response to ecosystem changes in the Barents Sea. Sarsia 87: 409-422

Haug T, Lindstrøm U, Nilssen KT, Røttingen I, Skaug HJ (1996) Diet and food availability for northeast Atlantic minke whales, *Balaenoptera acutorostrata*. Rep Int Whal Commn 46: 371-382

Horwood J (1990) Biology and exploitation of the minke whale. CRC Press, Inc., Boca Raton, Florida. 238 pp.

Ichii T, Shinohara N, Fujise Y, Nishiwaki S, Matsuoka K. (1998) Interannual changes in body fat condition index of minke whales in the Antarctic. Mar Ecol Prog Ser 175: 1-12

Ingvaldsen R, Gjøsæter H (2013) Responses in spatial distribution of Barents Sea capelin to changes in stock size, ocean temperature and ice cover. Mar Biol Res 9: 867-877. doi:10.1080/17451000.2013.775450

Johannesen E, Lindstrøm U, Michalsen K, Skern-Mauritzen M, Fauchald P, Bogstad B, Dolgov AV (2012) Feeding in a heterogeneous environment: spatial dynamics in summer foraging Barents Sea cod. Mar Ecol Prog Ser 458: 181-197. doi: 10.3354/meps09818

Jonsgård Å (1951) Studies on the little piked whale or minke whale. Norsk Hvalfangst-Tid 5: 210-233

Jonsgård Å (1966) The distribution of Balaenopteridae in the North Atlantic Ocean In: Norris KS (ed) Whales, Dolphins and Porpoises. University of Calfornia Press, Berkely, pp 114-124

Cohen J (1988) Statistical power analysis for the behavioral sciences (2nd ed.). New Jersey: Lawrence Erlbaum.

Konishi K, Tamura T, Zenitani R, Bando T, Kato H, Walløe L (2008) Decline in energy storage in the Antarctic minke whale (*Balaenoptera bonarensis*) in the Southern Ocean. Polar Biol 31: 1509-1520

Lindstrøm U, Haug T (2001) Feeding strategy and prey selectivity in common minke whales (*Balaenoptera acutorostrata*) foraging in Southern Barents Sea during early summer. J Cet Res Manage 3: 239-249

Lockyer C (1981) Growth and energy budgets of large baleen whales from the southern hemisphere. FAO Fish Ser 5: 379-487

Lockyer C (1986) Body fat condition in Northeast Atlantic fin whales, *Balaenoptera physalus*, and its relationship with reproduction and food resource. Can J Fish Aquat Sci 43: 142-147

Lockyer C, Mcconnell LC, Waters TD (1985) Body condition in terms of anatomical and biochemical assessment of body fat in North Atlantic fin and sei whales. Can J Zool 63: 2328-2338

Lockyer C, Waters TD (1986) Weights and anatomical measurements of northeastern Atlantic fin (*Balaenoptera physalus*, Linnaeus) and sei (*B. borealis*, Lesson) whales. Mar Mamm Sci 2: 169-185

McBride MM, Filin A, Titov O, Stiansen JE (Eds) (2014). IMR/PINRO update of the "Joint Norwegian-Russian environmental status report on the Barents Sea Ecosystem" giving the current situation for climate, phytoplankton, zooplankton, fish, and fisheries during 2012-13. IMR/PINRO Joint Report Series 1-2014, ISSN 1502-8828, 64 pp.

Michalsen K, Dalpadado P, Eriksen E, Gjøsæter H, Ingvaldsen RB, Johannesen E, Jørgensen LL, Knutsen T, Prozorkevich D, Skern-Mauritzen M (2013) Marine living resources of the Barents Sea – Ecosystem understanding and monitoring in a climate change perspective. Mar Biol Res 9: 932-947

Mitchell ED (1991) Winter records of the minke whale (*Balaenoptera acutorostrata* Lacépède 1804) in the southern North Atlantic. Rep Int Whal Commn 41: 455-457

Mori M, Butterworth DS (2006) A first step towards modeling the krill-predator dynamics of the Antarctic ecosystem. CCAMLR Sci 13: 217-277

Næss A, Haug T, Nilssen EM. (1998) Seasonal variation in body condition and muscular lipid contents in northeast Atlantic minke whales *Balaenoptera acutorostrata*. Sarsia 83: 211-218

Nilssen KT, Haug T, Grotnes PE, Potelov VA (1997) Seasonal variation in body condition of adult Barents Sea harp seals (*Phoca groenlandica*). J Northw Atl Fish Sci 22: 17-25

Nøttestad L, Krafft BA, Anthonypillai V, Bernasconi M, langård L, Mørk HL, Fernö A (2015) Recent changes in distribution and relative abundance of cetaceans in the Norwegian Sea and their relationship with potential prey. Front Ecol Evol 2:83. doi: 10.3389/fevo.2014.00083

Nøttestad L, Olsen E (2004) Whales and seals: top predators in the ecosystem. In: Skjoldal HR, Misund OA, Sætre R, Fernö A, Røttingen I (eds). The Norwegian Sea Ecosystem. Tapir Academic Press, Trondheim, pp 395-434

Øigård TA, Lindstrøm U, Haug T, Nilssen KT, Smout S (2013) Functional relationship between harp seal body condition and available prey in the Barents Sea. Mar Ecol Prog Ser 484: 287-301

Prokhorova T (Ed) (2013). Survey report from the joint Norwegian/Russian ecosystem survey in the Barents Sea August-October 2013. IMR/PINRO Joint Report Series, No. 4/2013. ISSN 1502-8828, 131 pp.

Satoh K, Yanagihara H (2010) Estimation of varying coefficients for a growth curve model. Amer J Math Management Sci 30: 243-256

Skern-Mauritzen M, Johannesen E, Bjørge A, Øien N (2011) Baleen whale distributions and prey associations in the Barents Sea. Mar Ecol Prog Ser 426: 289-301. doi:10.3354/09027

Stewart BS, Leatherwood S (1985) Minke whale, *Balaenoptera acutorostrata* Lacépède, 1804. In: Ridgway SH, Harrison R (eds). Handbook of marine mammals. Vol. 3 The Sirenians and Baleen Whales. Academic Press, London, pp 91-136

Timoshenko YK (1995) Harp seals as indicators of the Barents Sea ecosystem. Iin: Blix AS, Walløe L, Ulltang Ø (eds) Whales, seals, fish, and man. Elsevier Science BV, pp 509-526

Tonda T, Satoh K (2013) Improvement of confidence interval for linear varying coefficient. Japanese J Appl Statist 42: 11-21 (in Japanese)

Van Waerebeek K, André M, Sequeira M, Martín V, Robineau D, Collet A, Papastavrou V, Ndiaye E (1999) Spatial and temporal distribution of the minke whale, Balaenoptera acutorostrata (Lacépède, 1804), in the southern northeast Atlantic Ocean and the Mediterranean Sea, with reference to stock identity. J Cet Res Man 1: 223-237

Vikingsson G (1990) Energetic studies on fin and sei whales caught off Island. Rep Int Whal Commn 40: 365-373

Vikingsson G (1995) Body condition of fin whales during summer off Island. In: Blix AS, Ulltang Ø, Walløe L (eds) Whales, seals, fish and man. Elsevier, Science BV, pp 361-369

Wassmann P, Reigstad M, Haug T, Rudels B, Carroll ML, Hop H, Gabrielsen GW, Falk-Petersen S, Denisenko SG, Arashkevich E, Slagstad D, Pavlova O (2006) Food web and carbon flux in the Barents Sea. Prog Oceanogr 71: 232-287

West M, Harrison PJ, Migon HS (1985) Dynamic generalized linear models and Bayesian forcasting (with discussion). J Am Stat Ass 80: 73-97

Windsland K, Lindstrøm U, Nilssen KT, Haug T (2007) Relative abundance and size composition of prey in the common minke whale diet in selected areas of the northeast Atlantic during 2000-04. J Cet Res Man 9: 167-178

Legends to figures

Figure 1
Catch positions for common minke whales taken in commercial catch operations in Norwegian waters in the period from May to September, 1993-2013.

Figure 2
Positions of blubber thickness (BT1, BT2 and BT3) and half girth measurements on the common minke whales.

Figure 3
Common minke whale body condition data (blubber thickness BT1, BT2 and BT3, and Girth measurenments) versus year in the period 1993-2013.

Figure 4
Common minke whale body condition data (blubber thickness BT1, BT2 and BT3, and Girth measurements) versus year for seasons I (April-May), II (June-July) and III (August-September) in the period 1993-2013.

Figure 5
Estimated random effect of year and area for common minke whale blubber thickness measurements (BT1 and BT3) observed in season II (June-July).

Figure 6
Estimated variation coefficients (VC) of year (solid line: estimated VC, dotted line: the confidence intervals) and area (red lines means larger values effect than blue lines) for common minke whale blubber thickness measurements (BT1 and BT3) observed in season II (June-July).

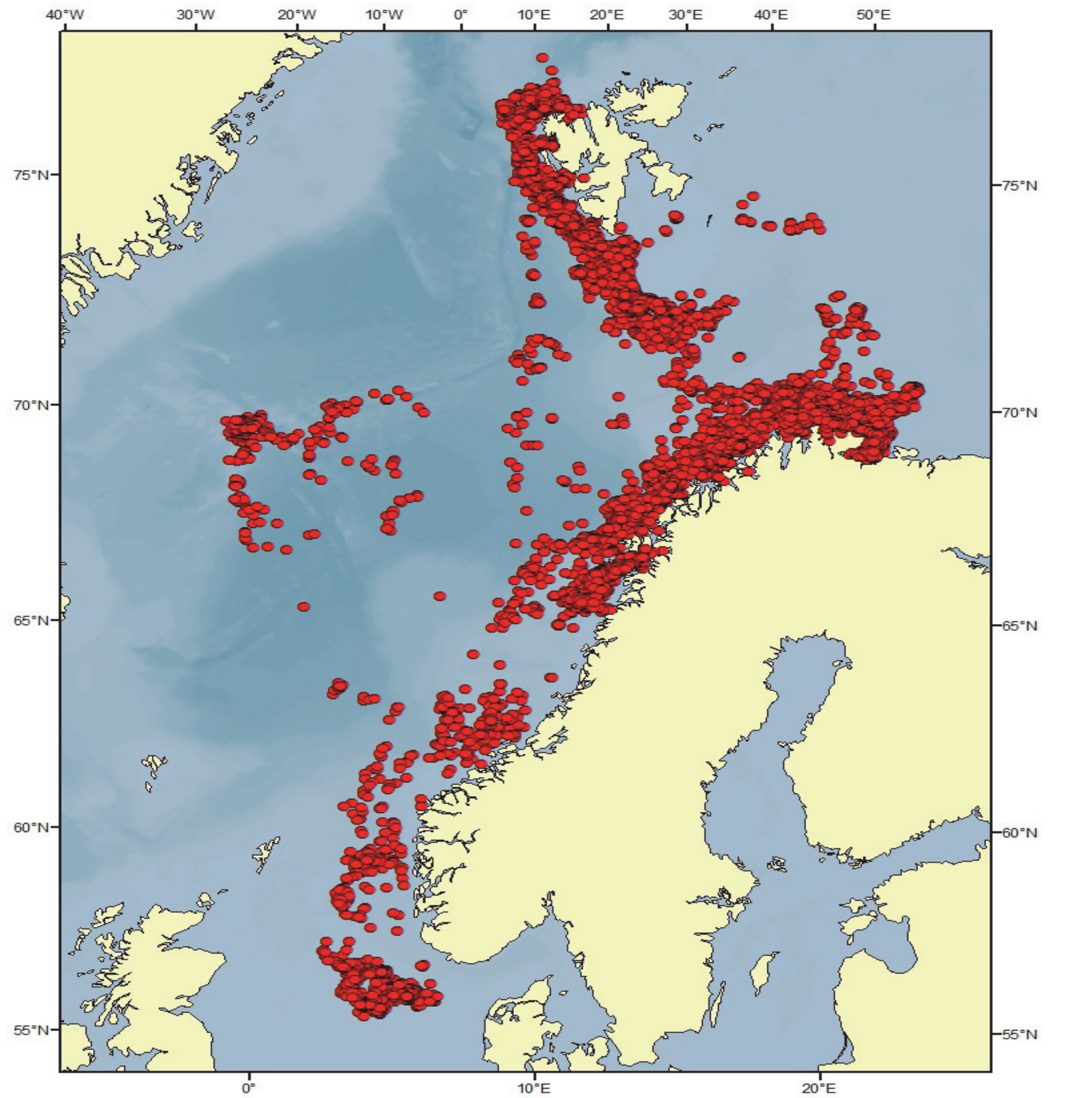
40°W
30°W
20°W
10°W
0°
10°E
20°E
30°E
40°E
50°E
75°N
70°N
65°N
60°N
55°N
0°
10°E
20°E

Fig. 1.

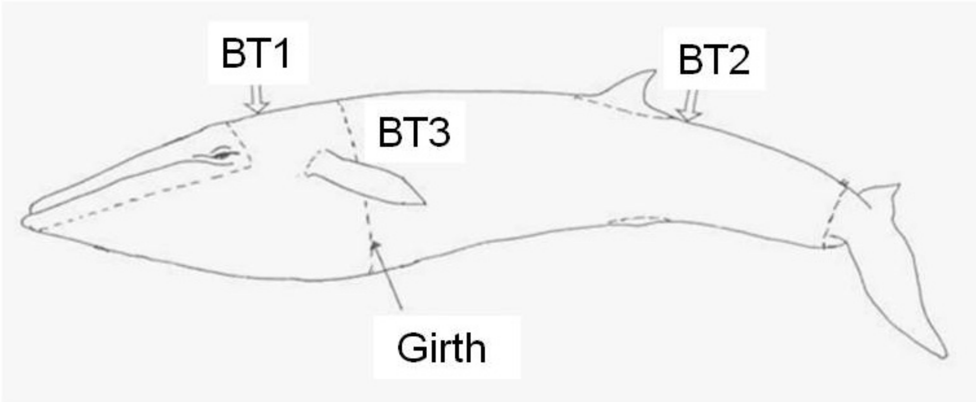

Fig. 2.

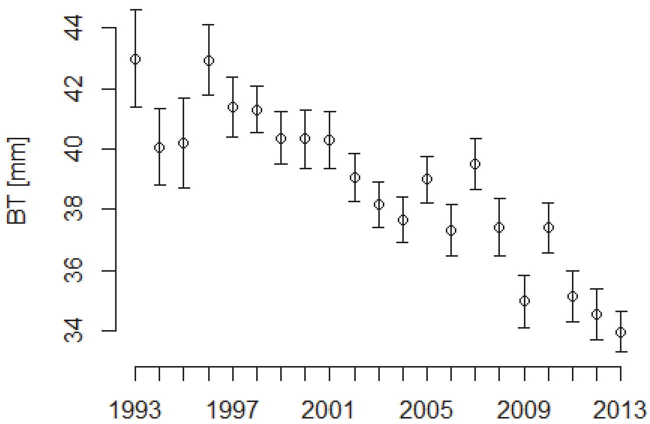

BT1

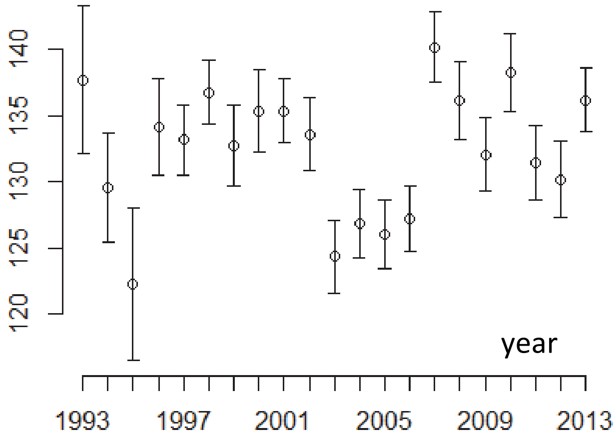

BT2

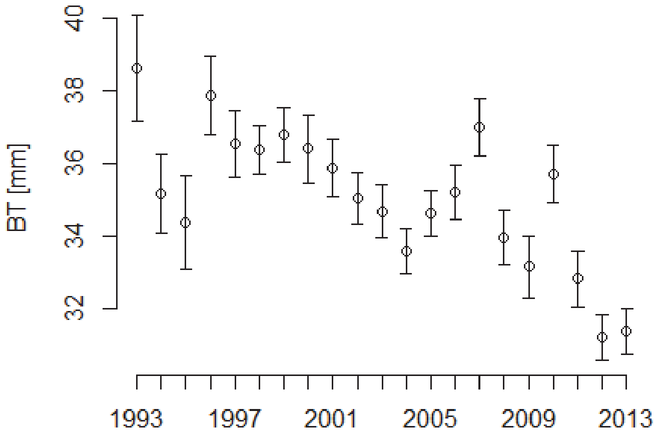

BT3

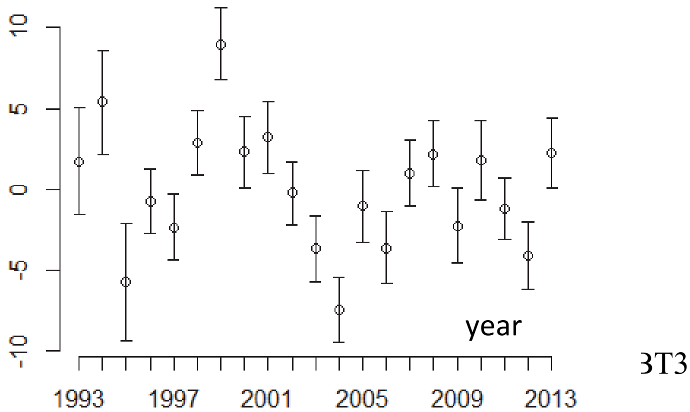

Girth

Fig.3

BT1 BT2

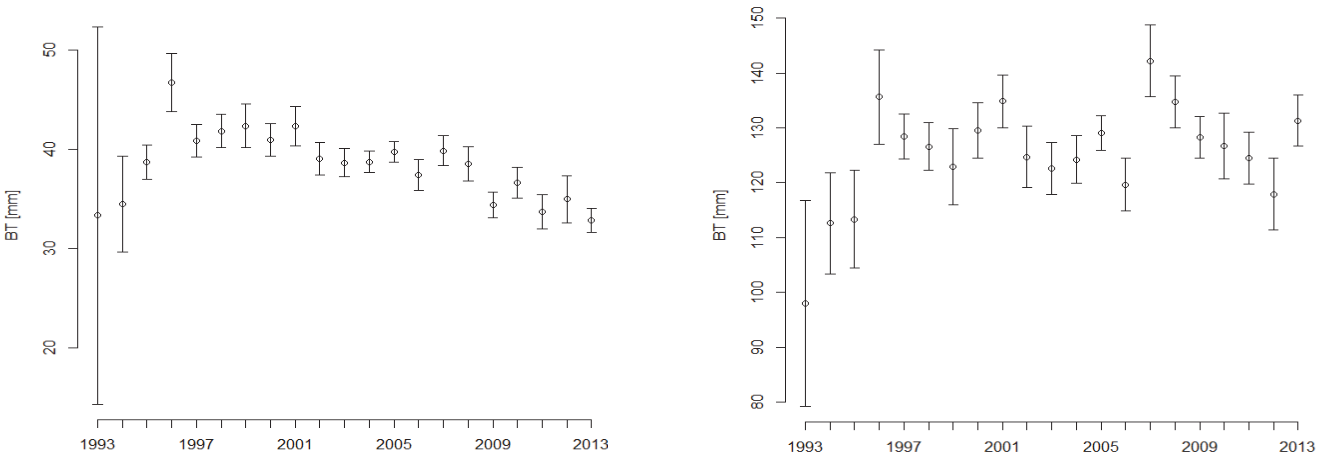

Season I (April and May)

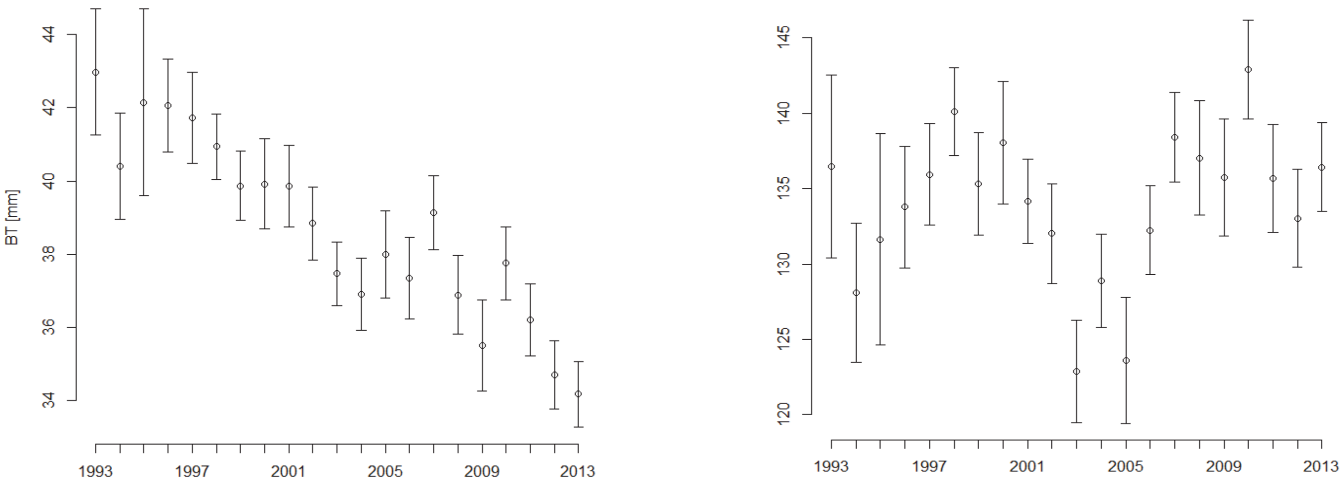

Season II (June and July)

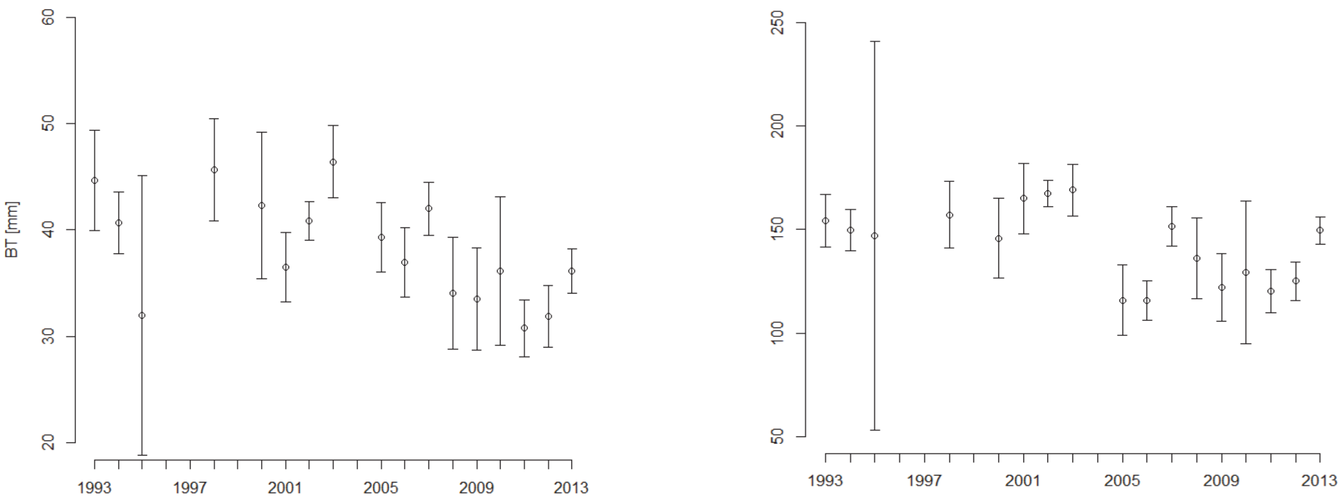

Season III (August and September)

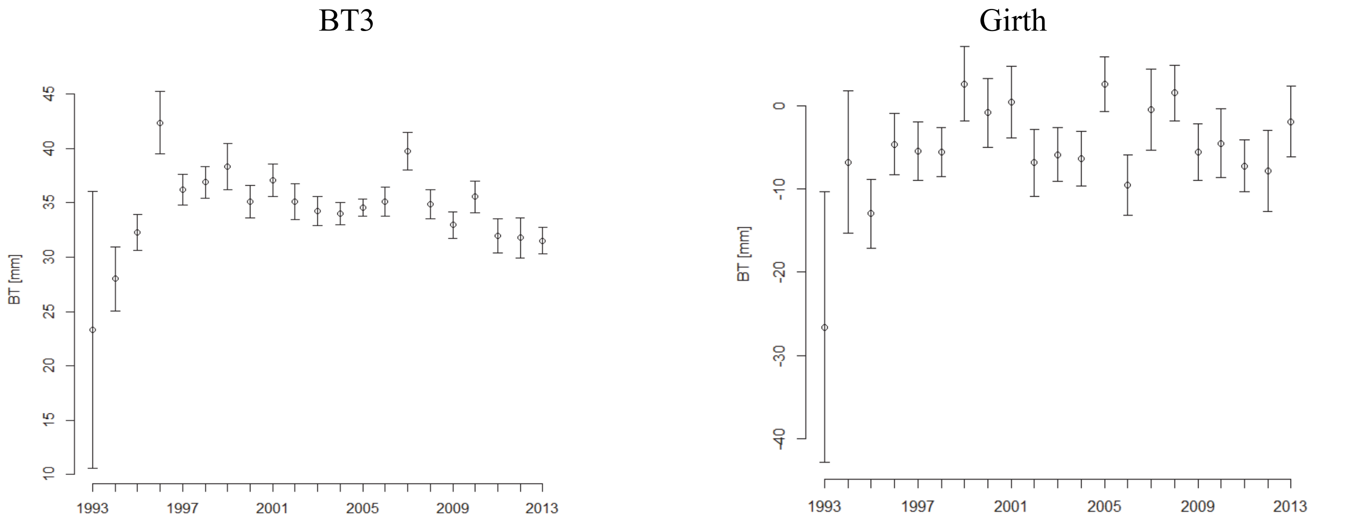

Season I (April and May)

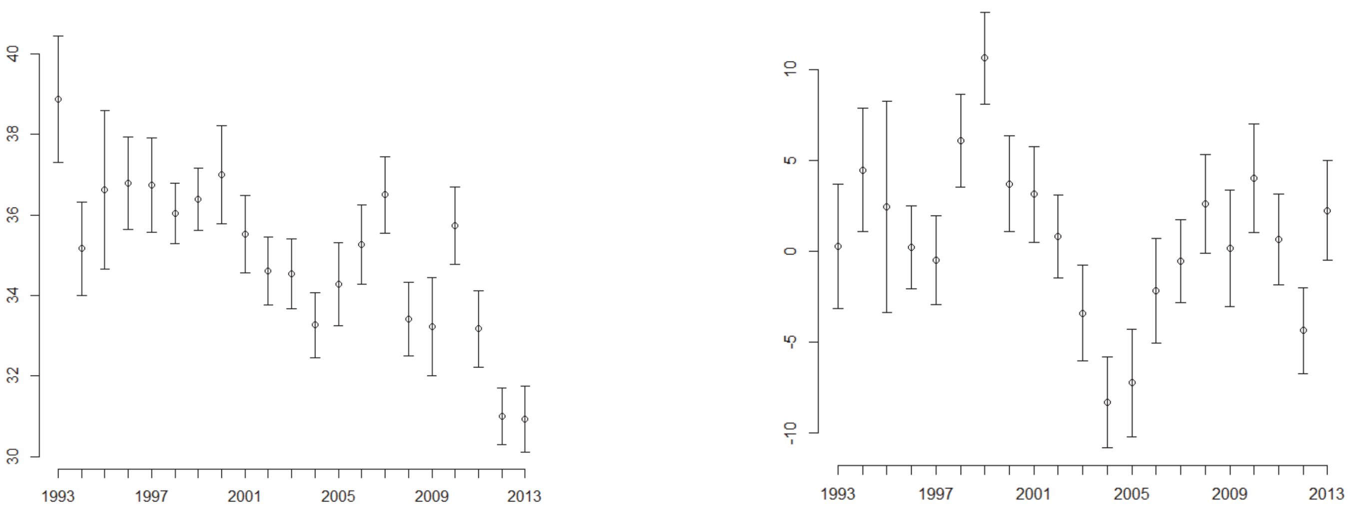

Season II (June and July)

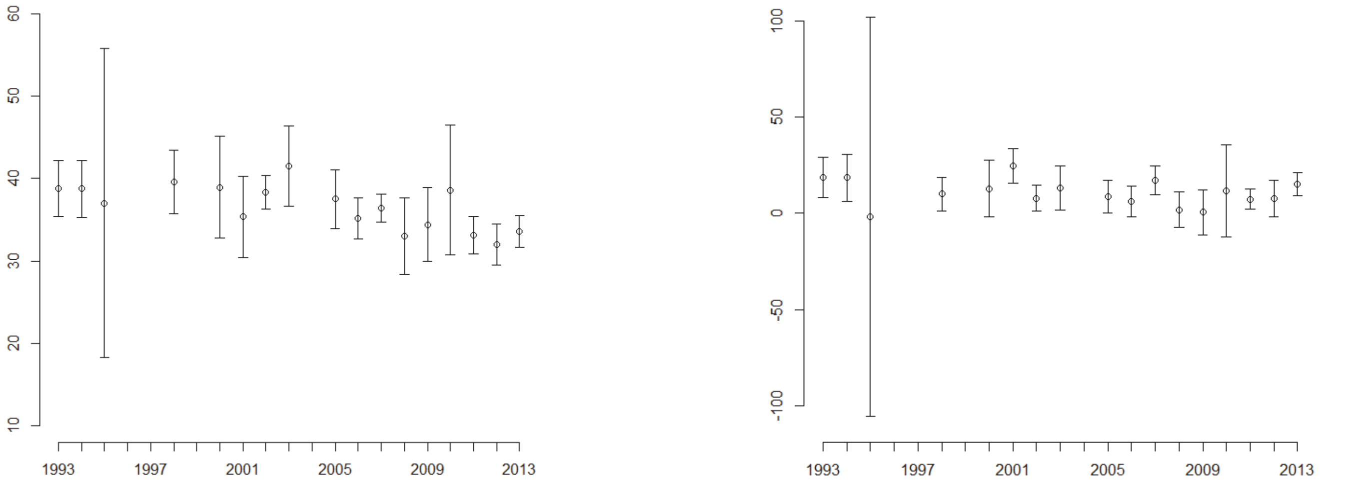

Season III (August and September)

Fig. 4

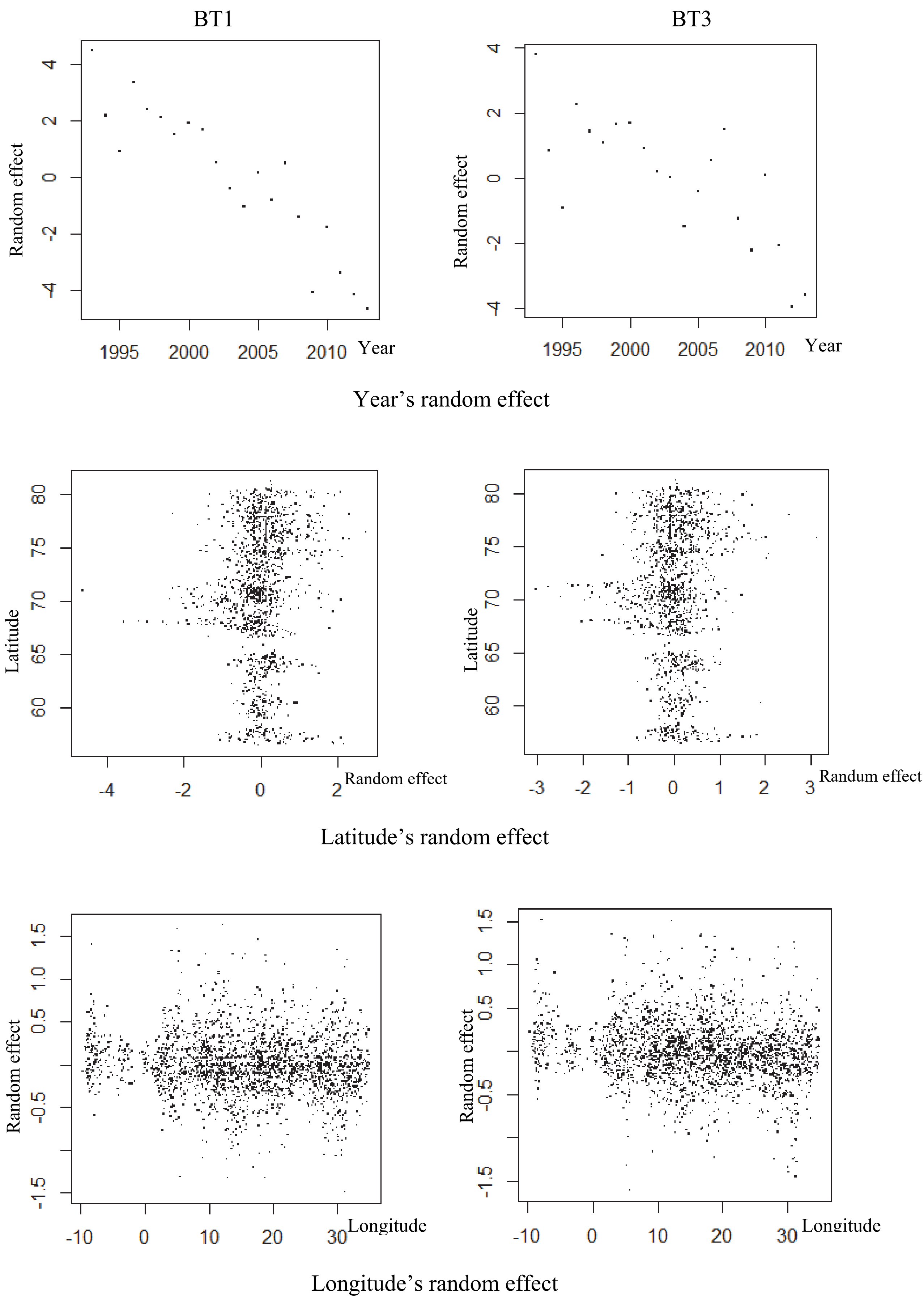
BT1
BT3
Random effect
Year
1995
2000
2005
2010
Year's random effect
Latitude
Random effect
Randum effect
Latitude's random effect
Random effect
Longitude
Longitude's random effect

Fig. 5

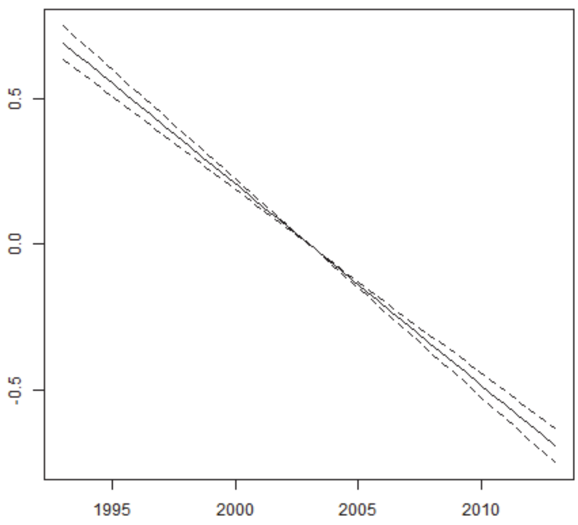

VC (p=1) of year for BT1

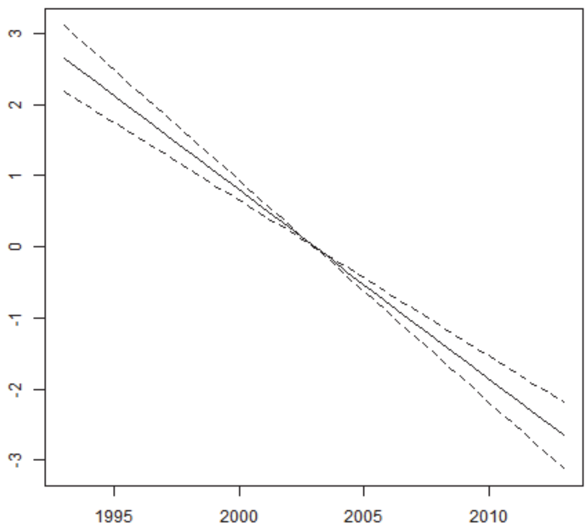

VC (p=3) of year for BT3

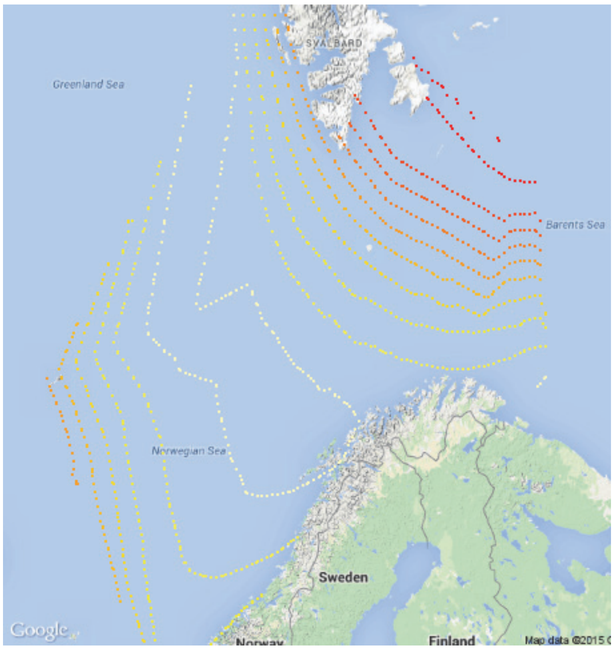

VC (q=3) of areas for BT1

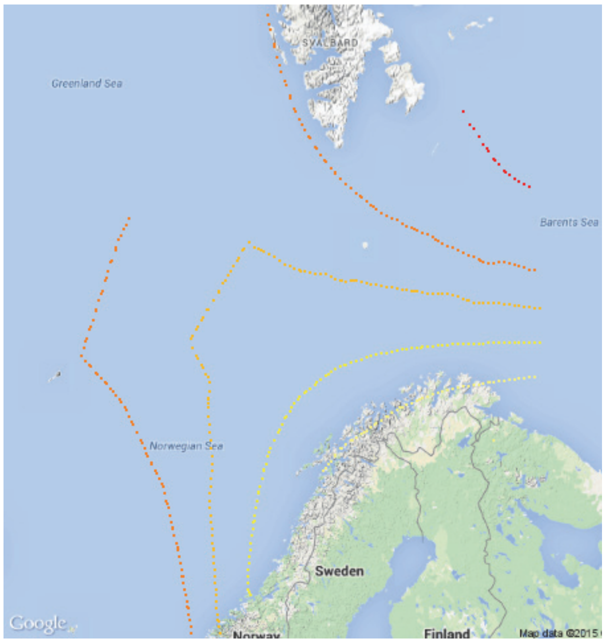

VC(q=2) of areas for BT3

Fig. 6

Table 1. Number of individuals by season (April and May as season I, June and July as season II and August and September as season III) for each sampling year.

BT1							
year	season I		season II		season III		Total
	male	female	male	female	male	female	
1993	0	3	71	100	13	7	194
1994	2	15	110	114	19	12	272
1995	13	100	19	81	2	1	216
1996	2	72	51	256	0	0	381
1997	19	162	94	220	0	0	495
1998	27	146	92	332	9	8	614
1999	24	91	137	304	0	0	556
2000	30	120	129	154	10	2	445
2001	9	120	171	222	15	3	540
2002	26	109	169	255	31	24	614
2003	51	167	149	246	14	8	635
2004	37	190	118	186	0	0	531
2005	33	304	96	158	24	13	628
2006	48	107	147	188	24	20	534
2007	29	56	103	320	26	25	559
2008	47	148	117	199	4	9	524
2009	57	147	60	203	8	9	484
2010	8	118	89	240	3	4	462
2011	23	125	113	218	25	8	512
2012	11	56	108	236	22	6	439
2013	48	120	101	247	37	19	572
Total	544	2476	2244	4479	286	178	10207

BT2							
year	season I		season II		season III		Total
	male	female	male	female	male	female	
1993	0	3	70	100	13	7	193
1994	2	15	110	114	19	12	272
1995	13	100	19	81	2	1	216
1996	2	72	51	256	0	0	381
1997	19	163	94	220	0	0	496
1998	27	146	92	332	9	8	614
1999	24	91	137	302	0	0	554
2000	30	120	129	152	10	2	443
2001	9	120	170	222	15	3	539
2002	26	108	169	255	31	24	613
2003	51	167	151	246	14	8	637
2004	37	192	118	186	0	0	533
2005	33	304	97	158	24	13	629
2006	48	107	147	188	24	20	534
2007	29	56	103	320	26	25	559

2008	47	148	117	199	4	9	524
2009	57	147	60	203	8	9	484
2010	8	118	89	240	3	4	462
2011	23	125	113	218	25	8	512
2012	11	56	108	236	22	6	439
2013	48	120	101	244	37	19	569
Total	544	2478	2245	4472	286	178	10203

BT3

year	season I		season II		season III		Total
	male	female	male	female	male	female	
1993	0	3	71	100	13	7	194
1994	2	13	110	114	19	12	270
1995	13	100	19	81	2	1	216
1996	2	72	51	256	0	0	381
1997	19	163	94	220	0	0	496
1998	27	146	92	331	9	8	613
1999	24	91	137	303	0	0	555
2000	29	117	129	153	10	2	440
2001	9	120	171	222	15	3	540
2002	26	109	169	254	31	24	613
2003	51	166	151	245	14	8	635
2004	37	192	118	186	0	0	533
2005	33	304	97	158	24	13	629
2006	48	107	147	188	24	20	534
2007	29	56	103	320	26	25	559
2008	47	148	117	199	4	9	524
2009	57	147	60	203	8	9	484
2010	8	118	89	240	3	4	462
2011	23	125	113	218	25	8	512
2012	11	56	108	236	22	6	439
2013	48	120	100	246	37	19	570
Total	543	2473	2246	4473	286	178	10199

Girth

year	season I		season II		season III		Total
	male	female	male	female	male	female	
1993	0	3	71	100	13	7	194
1994	2	15	110	114	19	12	272
1995	13	100	19	81	2	1	216
1996	2	72	51	257	0	0	382
1997	19	163	94	220	0	0	496
1998	27	146	92	332	9	8	614
1999	24	92	137	304	0	0	557
2000	33	133	131	156	10	2	465
2001	9	120	171	221	15	3	539
2002	26	108	169	256	31	24	614

2003	50	167	151	246	14	8	636
2004	37	195	118	186	0	0	536
2005	33	305	97	158	24	13	630
2006	47	105	147	188	24	20	531
2007	36	59	108	326	26	25	580
2008	47	149	117	200	4	9	526
2009	57	147	60	203	8	9	484
2010	8	118	90	241	3	4	464
2011	23	127	115	228	25	9	527
2012	11	67	108	238	25	7	456
2013	49	121	106	251	38	19	584
Total	553	2512	2262	4506	290	180	10303

Table 2. Summary for fitting models. 1|* indicates random effect of intercept for covariate. * indicates model selected by minimum BIC.

Models		# parameters	BT1		BT2	
			log-likelihood	BIC	log-likelihood	BIC
OLM	sex (s)	2	-38091.35	76210.39	-50080.68	100189.05
	year (y)	2	-38078.39	76184.47	-50132.12	100291.94
	longitude (lo)	2	-38290.92	76609.53	-49953.18	99934.04
	latitude (la)	2	-38297.93	76623.55	-50131.47	100290.64
	s + y	3	-37844.01	75724.94	-50079.94	100196.80
	la + lo	3	-38253.16	76543.25	-49933.03	99902.97
	s+ la	3	-38091.27	76219.46	-50079.56	100196.04
	s + lo	3	-38062.47	76161.87	-49900.69	99838.31
	y + la	3	-38036.33	76109.57	-50131.04	100298.99
	y + lo	3	-38040.61	76118.15	-49953.11	99943.14
	y + la + lo	4	-37972.24	75990.63	-49932.95	99912.05
	s + la + lo	**4**	-38059.64	76165.44	**-49894.92**	**99835.99***
	s + y + la + lo	**5**	**-37791.33***	**75638.05***	-49894.92	99845.22
	Best + d1 + d2	7	-37782.20	75638.26	-49823.68	99711.97
REM	1|y	2	-38073.17	76174.04	-50064.81	100157.32
	1|lo	2	-38298.37	76624.44	-50045.85	100119.38
	1|la	2	-38243.86	76515.41	-49909.96	99847.61
	s + 1|y	3	-37844.06	75725.05	-50012.18	100061.29
	s + 1|lo	3	-38076.48	76189.88	-49993.66	100024.25
	s + 1|la	3	-38048.70	76134.33	-49881.83	99800.59
	s + 1|y + 1|la	**4**	**-37811.31**	**75668.78***	-49833.38	99712.91
	s + 1|la + 1|lo	4	-38042.14	76130.44	-49859.89	99765.93
	s + 1|y + 1|lo	4	-37835.13	75716.42	-49942.53	99931.21
	s + 1|y + 1|la + 1|lo	5	-37806.74	75668.86	**-49815.29**	**99685.96***
	Best + d1 + d2	7	-37796.18	75608.36	-49721.70	99459.39
VCM	p=1, q=2	5	-37711.76	75506.60	-49686.25	99455.57
	p=1, q=3	6	-37689.85	75499.70	-49680.58	99481.16
	p=1, q=4	7	-37686.64	75539.44	-49663.92	99493.98
	p=2, q=1	5	-37781.83	75628.27	-49891.13	99846.87
	p=3, q=1	6	-37781.82	75628.26	-49888.31	99850.46
	p=4, q=1	7	-37781.67	75637.19	-49887.23	99857.53
	p=2, q=2	6	-37703.32	75498.95	**-49680.57**	**99453.45***
	p=2, q=3	**7**	**-37679.63**	**75488.48***	-49675.51	99480.25
	p=2, q=4	8	-37677.12	75529.63	-49658.33	99492.03
	p=3, q=2	7	-37702.15	75505.83	-49680.12	99461.77
	p=4, q=2	8	-37701.90	75514.57	-49679.80	99470.37
	p=3, q=3	8	-37678.97	75496.40	-49674.88	99488.22
	p=3, q=4	9	-37676.08	75536.78	-49658.04	99500.69
	p=4, q=3	9	-37678.39	75504.47	-49674.72	99497.14

	p=4, q=4	10	-37675.79	75545.42	-49657.71	99509.26
	Best + d1 + d2		-37665.45	75478.60	-49581.53	99273.82

Models		# parameters	BT3		Girth	
			log-likelihood	BIC	log-likelihood	BIC
OLM	sex (s)	2	-36856.37	73740.42	-47874.92	95777.57
	year (y)	2	-36935.07	73897.83	-47906.86	95841.44
	longitude (lo)	2	-36981.98	73991.65	-47783.48	95594.68
	latitude (la)	2	-37036.70	74101.09	-47873.22	95774.16
	s + y	3	-36742.70	73522.32	-47870.09	95777.13
	la + lo	3	-36952.87	73942.65	-47770.56	95578.09
	s+ la	3	-36855.69	73748.31	-47804.51	95645.98
	s + lo	3	-36789.93	73616.78	-47746.49	95529.94
	y + la	3	-36915.08	73867.07	-47870.27	95777.50
	y + lo	3	-36860.64	73758.21	-47775.57	95588.10
	y + la + lo	4	-36814.04	73674.23	-47764.54	95575.27
	s + la + lo	**4**	-36788.33	73622.80	**-47713.87**	**95473.94***
	s + y + la + lo	**5**	**-36659.77**	**73374.92***	-47709.34	95474.13
	Best + d1 + d2	7	-36637.25	73348.33	-47613.58	95291.83
REM	1|y	2	-36886.22	73800.12	-47835.35	95698.43
	1|lo	2	-37035.28	74098.26	-47859.25	95746.21
	1|la	2	-37007.66	74043.02	-47848.21	95724.14
	s + 1|y	3	-36693.53	73423.99	-47794.17	95625.30
	s + 1|lo	3	-36847.44	73731.81	-47820.72	95678.39
	s + 1|la	3	-36838.25	73713.42	-47812.95	95662.86
	s + 1|y + 1|la	4	-36667.39	73380.92	-47741.79	95529.78
	s + 1|la + 1|lo	4	-36831.19	73708.53	-47787.00	95620.19
	s + 1|y + 1|lo	4	-36684.32	73414.80	-47751.72	95549.63
	s + 1|y + 1|la + 1|lo	**5**	**-36661.56**	**73378.51***	**-47721.98**	**95499.41***
	Best + d1 + d2	7	-36636.71	73347.26	-47611.69	95297.30
VCM	p=1, q=2	5	-36627.09	73337.24	-47647.64	95378.43
	p=1, q=3	6	-36616.01	73352.00	-47643.47	95407.06
	p=1, q=4	7	-36607.65	73381.45	-47632.35	95431.03
	p=2, q=1	5	-36646.85	73358.31	-47702.86	95470.41
	p=3, q=1	6	-36642.27	73358.38	-47695.93	95465.78
	p=4, q=1	7	-36641.65	73366.38	-47695.90	95474.96
	p=2, q=2	6	-36614.88	73322.06*	**-47641.19**	**95374.78***
	p=2, q=3	7	-36602.64	73334.51	-47637.42	95404.20
	p=2, q=4	8	-36592.72	73360.81	-47626.24	95428.05
	p=3, q=2	**7**	**-36609.01**	**73319.55***	-47637.27	95376.17
	p=4, q=2	8	-36608.55	73327.86	-47637.22	95385.32
	p=3, q=3	8	-36597.73	73333.91	-47633.06	95404.72
	p=3, q=4	9	-36589.01	73362.62	-47622.61	95430.03
	p=4, q=3	9	-36597.47	73342.63	-47632.98	95413.80

	p=4, q=4	10	-36588.84	73371.51	-47622.56	95439.15
	Best + d1 + d2		-36584.94	73280.64	-47531.45	95173.78

Table 3. Estimated parameters for time and areas in the best fit OLM and REM.

Model	Term	BT1	BT2	BT3	Girth
OLM (Coef)	Year	-0.42	-	-0.26	-
	Longitude	-0.10	-0.64	-0.12	-0.34
	Latitude	0.099	0.21	0.064	-0.37
REM (Variance)	1|year	6.7	15.6	3.9	12.4
	1|longitude	-	39.4	1.6	27.7
	1|latitude	3.2	94.5	2.2	25.7
VCM ($T_{h,\max} > \tau_\alpha$)	Year	21.9 > 2.4	3.6 > 2.4	13.1 > 2.6	3.3 > 2.4
	Area	3.9 > 2.0	20.5 > 2.0	7.4 > 2.0	9.1 > 2.0

Table 4. Summary for fitting models to BT1 and BT3 for season II. 1|* indicates random effect of intercept for covariate. * indicates selected model by minimum BIC

Models		# parameters	BT1		BT3	
			log-likelihood	BIC	log-likelihood	BIC
OLM	sex (s)	2	-25045.98	50118.41	-24240.89	48508.22
	year (y)	2	-25065.87	50158.18	-24314.01	48654.46
	longitude (lo)	2	-25187.48	50401.40	-24354.56	48735.56
	latitude (la)	2	-25205.08	50436.60	-24392.03	48810.50
	s + y	3	-24886.87	49808.99	-24149.43	48334.12
	la + lo	3	-25173.76	50382.77	-24340.63	48716.51
	s+ la	3	-25043.53	50122.32	-24237.66	48510.57
	s + lo	3	-25028.64	50092.53	-24206.81	48448.88
	y + la	3	-25041.77	50118.79	-24297.88	48631.02
	y + lo	3	-25036.62	50108.49	-24266.46	48568.17
	y + la + lo	4	-24997.75	50039.56	-24234.50	48513.06
	s + la + lo	4	-25028.29	50100.65	-24206.64	48457.34
	s + y + la + lo	**5**	**-24861.69**	**49776.26***	**-24108.79**	**48270.45***
REM	1|y	2	-25078.60	50183.63	-24292.03	48610.50
	1|lo	2	-25193.55	50413.54	-24386.79	48800.02
	1|la	2	-25168.36	50363.15	-24368.67	48763.79
	s + 1|y	3	-24904.48	49844.22	-24127.22	48289.70
	s + 1|lo	3	-25031.33	50097.91	-24232.56	48500.37
	s + 1|la	3	-25021.41	50078.08	-24227.88	48491.01
	s + 1|y + 1|la	4	-24887.24	49818.54	-24110.35	48264.76
	s + 1|la + 1|lo	4	-25013.14	50070.34	-24220.54	48485.14
	s + 1|y + 1|lo	4	-24897.13	49838.32	-24118.79	48281.65
	s + 1|y + 1|la + 1|lo	**5**	**-24882.46**	**49817.79***	**-24103.93**	**48260.74***
VCM	p=1, q=2	5	-24789.02	49657.35	-24075.01	48229.32
	p=1, q=3	**6**	**-24765.29**	**49645.16***	-24062.43	48239.43
	p=1, q=4	7	-24762.96	49684.56	-24051.21	48261.04
	p=2, q=1	5	-24860.60	49782.90	-24100.61	48262.91
	p=3, q=1	6	-24859.76	49790.02	-24093.07	48256.65
	p=4, q=1	7	-24859.15	49797.62	-24092.54	48264.39
	p=2, q=2	6	-24787.74	49663.62	-24066.39	48220.91
	p=2, q=3	7	-24762.43	49648.24	-24051.40	48226.18
	p=2, q=4	8	-24760.27	49687.99	-24038.80	48245.04
	p=3, q=2	7	-24784.57	49666.09	**-24056.13**	**48209.20***
	p=4, q=2	8	-24784.16	49674.08	-24055.65	48217.06
	p=3, q=3	8	-24760.75	49653.71	-24043.70	48219.59
	p=3, q=4	9	-24758.62	49693.51	-24033.11	48242.47
	p=4, q=3	9	-24760.75	49662.51	-24043.59	48228.18
	p=4, q=4	10	-24758.62	49702.32	-24033.10	48251.27

Table 5. Estimated parameters for time and areas in the best fit OLM and REM with seasonal effect.

Model	Term	BT1	BT3
OLM (Coef)	Year	-0.40	-0.27
	Longitude	-0.086	-0.099
	Latitude	0.065	0.046
REM (Variance)	Year	6.1	4.1
	Longitude	2.7	2.5
	Latitude	2.9	2.4
VCM ($T_{h,\max} > \tau_{\alpha}$)	Year	16.6 > 2.0	2.7 > 2.0
	Area	8.4 > 2.0	8.1 > 2.0